

Nested Polyhedra of MX_2 ($\text{M} = \text{W}, \text{Mo}$; $\text{X} = \text{S}, \text{Se}$) Probed by High-Resolution Electron Microscopy and Scanning Tunneling Microscopy

M. Hershfinkel,[†] L. A. Gheber,[†] V. Volterra,[†] J. L. Hutchison,[‡] L. Margulis,[§] and R. Tenne^{*§}

Contribution from the Department of Physics, Ben-Gurion University, P.O. Box 653, 84105 Beer-Sheva, Israel, Department of Materials, University of Oxford, Parks Road, Oxford OX1 3PH, U.K., and Department of Materials and Interfaces, Weizmann Institute, Rehovot 76100, Israel

Received September 7, 1993[®]

Abstract: Extensive investigation of the newly discovered fullerene-like nested polyhedra (NP) and nanotubules of metal dichalcogenides by scanning tunneling microscopy (STM) and high-resolution transmission electron microscopy is reported. Long-term spontaneous (room temperature) and electron beam assisted crystallization of amorphous precursor into NP or MX_2 ($\text{M} = \text{W}, \text{Mo}$; $\text{X} = \text{S}, \text{Se}$) was observed. This, along with other findings, suggests that the NP constitute a new metastable phase between the starting amorphous material and the thermodynamically stable bulk 2H allotrope. Characterization of the apex angles by STM suggests that the apexes of the NP may contain geometrical elements such as triangles and rhombuses, which do not exist in nested carbon fullerenes. The energy bandgap of the NP, determined using STM, was found to be somewhat smaller than that of the bulk 2H phase, and possible explanations for that phenomenon are forwarded.

Introduction

Layered metal dichalcogenides are anisotropic materials with trigonal prismatic structure, formed by stacking sandwiches consisting of a layer of transition-metal atoms between two layers of sulfur or selenium atoms. Their stable polytype at ambient conditions is the 2H one with hexagonal packing of layers in the sequence AbA BaB.¹ Small clusters of such compounds are expected to be unstable due to the large surface energy associated with dangling bonds at the peripheral atoms, and consequently folding into closed polyhedra will occur. Recently, fullerene-like nested polyhedra (NP) and nanotubules were described in the layered compound WS_2 ,^{2a} and NP were also found in MoS_2 .^{2b} Among apex angles, observed by transmission electron microscopy (TEM), those of $\leq 90^\circ$ have no counterpart in carbon fullerenes. These angles were ascribed to the folding of the hexagonal network of atoms around triangular and rhombic polygons which form part of the 2H- MX_2 stable structure.^{2b} It was suggested^{2b} that closed polyhedra of MoS_2 are formed as an intermediate metastable "phase" during the sequence of chemical and structural transformations which converts the starting material, amorphous MoO_x ($x \sim 3$) into the stable 2H- MoS_2 crystalline phase.

In this report, scanning tunneling microscopy (STM) and TEM were used to observe NP and nanotubules in metal dichalcogenides and to elucidate the growth mechanism and structure of MX_2 ($\text{M} = \text{W}, \text{Mo}$; $\text{X} = \text{S}, \text{Se}$) NP. While TEM images are obtained from a sequence of atomic planes within the bulk, STM probes the morphology of the outermost plane of the crystallite. Furthermore, TEM can probe curved surfaces with atomic resolution, while the resolution of the STM is hampered at nonflat surfaces, in general.³ Initial information on the electrical properties of these structures has also been obtained using the STM.

The chalcogenide atoms at the van der Waals (vdW) (0001) surface of MX_2 compounds are covalently bonded to the metal atom, leaving no free electrons in dangling bonds. Hence the vdW surface is inert to the surrounding atmosphere. Consequently, STM and atomic force microscopy (AFM) have been extensively used to image bulk 2H- MX_2 surfaces with atomic resolution in ambient conditions (see, for example, refs 4 and 5).

Experimental Section

MS_2 samples were prepared by annealing thin (60 nm) molybdenum (tungsten) oxide films on a quartz substrate in $\text{H}_2\text{S}/\text{H}_2/\text{N}_2$ gas atmosphere for 30 min at 850 °C. A similar procedure was used to prepare NP of the type MSe_2 , with selenium gas atmosphere replacing H_2S . After annealing, the films were peeled off from the substrate and transferred onto Cu grids. Both homemade and commercial instruments were used for the STM experiments and produced similar results. STM images were taken in the constant current (topographic) mode. Tunneling currents in the range of 1 nA and bias voltages in the range of 1 V were used, the bias polarity having little influence on the quality of the images. Tips were mechanically cut from Pt-Ir wires (0.25-mm diameter). Electrical contact was provided by silver paint. TEM analyses were performed initially with conventional TEM (CTEM) at 120 keV and subsequently with a high-resolution TEM (HRTEM) at 400 keV.

Results and Discussion

Figure 1a shows a HRTEM image of WS_2 fullerene-like NP with almost a spherical shape. The concentric rings in the outer part of the image are projections of the basal planes parallel to the beam. In the center of the polyhedron, an atomic arrangement of six-fold symmetry is observed. This arrangement is a fingerprint of basal planes which are perpendicular to the electron beam. Since this general pattern is preserved upon tilting the sample within the microscope, it confirms the closed nature of these structures. Furthermore, selected area electron diffraction of such structures contains simultaneously $\{00.l\}$ and $\{hk.0\}$ reflections, which is an independent confirmation of the closed nature of the polyhedra.^{2a} The lattice constants, measured directly from

* Author to whom correspondence should be addressed.

[†] Ben-Gurion University.

[‡] University of Oxford.

[§] Weizmann Institute.

[®] Abstract published in *Advance ACS Abstracts*, February 1, 1994.

(1) Wilson, J. A.; Yoffe, A. D. *Adv. Phys.* 1969, 18, 193.

(2) (a) Tenne, R.; Margulis, L.; Genut, M.; Hodes, G. *Nature* 1992, 360, 444. (b) Margulis, L.; Salitra, G.; Talianker, M.; Tenne, R. *Nature* 1993, 365, 113.

(3) Weaver, J. H. *Acc. Chem. Res.* 1992, 25, 143.

(4) Parkinson, B. A. *J. Am. Chem. Soc.* 1990, 112, 1030.

(5) Manivannan, A.; Hoshi, H.; Nagahara, L. A.; Mori, Y.; Maruyama, Y.; Kikuchi, K.; Achiba, Y.; Fujishima, A. *Jpn. J. Appl. Phys.* 1992, 31, 3680.

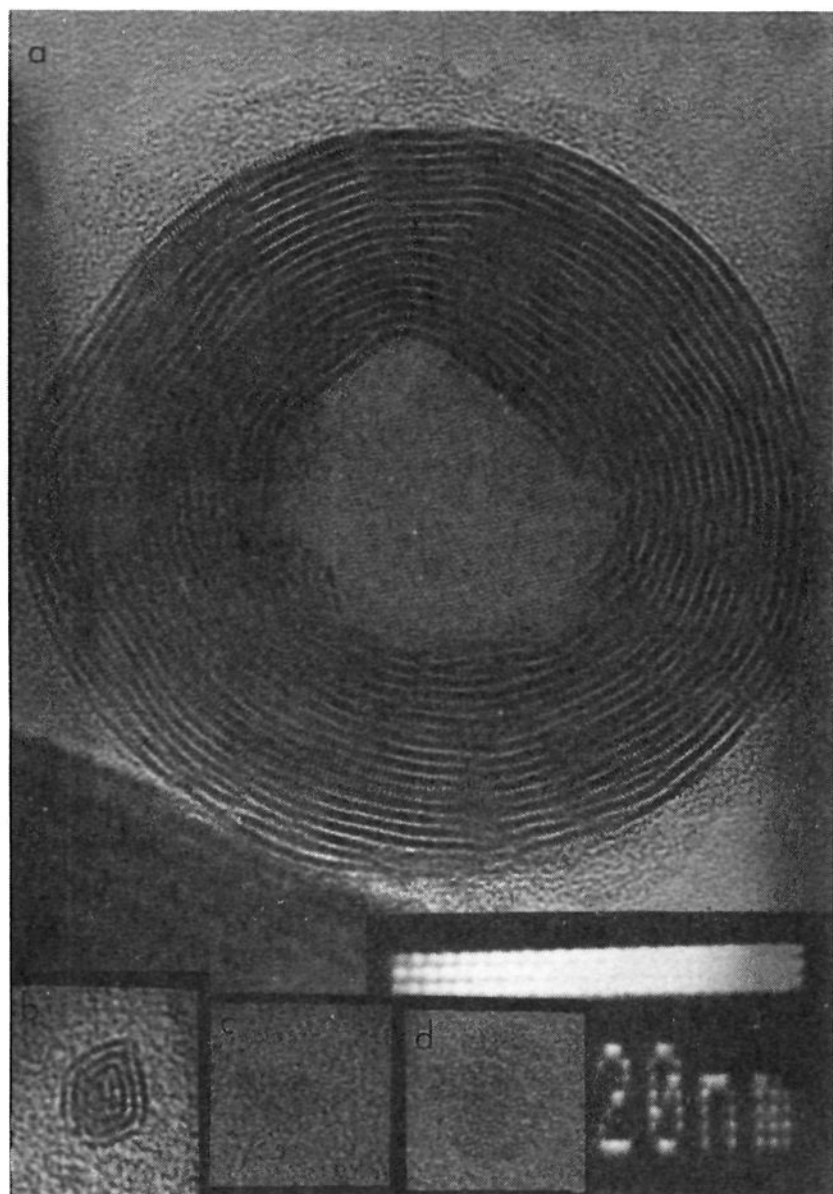


Figure 1. (a) HRTEM image of a typical WS_2 NP. Edge dislocations and loci where the vdW gap (c/w) has expanded are observed. The 20-nm bar gives the scale for this image only. (b) WS_2 polyhedron which crystallized from an amorphous matrix spontaneously during 22 months at room temperature. Note the icospiral-like growth and the sharp angles ($<90^\circ$) in a few corners. The average distance between the layers ($c/2$) is 0.62 nm. (c) Embryo (ca. 5 nm in diameter) which was produced during this period of time. (d) The same embryo after ca. 20 min of electron beam irradiation (400 keV). The average distance between the two fringes ($c/2$) is 0.62 nm.

images and calculated from selected area electron diffraction, are $a = 0.33$ nm, $c = 0.62$ nm and agree with published values.¹ Edge dislocations (i.e., truncated atomic planes) and other imperfections are repetitively observed in these structures. The almost symmetric "corona" around the NP is an amorphous material which started, but did not complete, crystallization.

Annealing of amorphous MO_x ($x \sim 3$) film in the reducing atmosphere of $H_2S/H_2/N_2$ gas yields first amorphous MS_x film. Further annealing converts it into bulk 2H- MS_2 crystal, which is the thermodynamically stable phase.^{2b} Presumably, the NP appear as a metastable intermediate phase in this latter process. The transformation of amorphous WX_x into NP is demonstrated in Figures 1b–d. One of the first samples used in the initial report^{2a} was kept in a drawer and periodically examined by CTEM. After 1 year, many tiny clusters appeared in the amorphous WS_x matrix. Some of them slowly developed into nuclei of NP. Lattice image of such a nucleus with 0.62-nm distance between atomic planes is shown in Figure 1b (after 22 months). Tilting experiments clearly confirmed the closed nature of this nanocrystallite. The growth of the small NP can be possibly described as an icospiral nucleation, in which case accretion of ever larger shells (layers with more hexagons) leads to escargot-shaped crystallites.^{6,7}

Twenty-four months after production, this sample was examined by a HRTEM. It was noticed that the irradiation of the

amorphous WS_x matrix with the electron beam produced more nuclei of NP within 10–20 min. The size and degree of crystallinity depended of the duration of the process. Partially crystallized NP nuclei with an incomplete round shape, which exhibited residual diffraction contrast, were observed in various regions of the sample. Figure 1c shows an image of a typical embryo (ca. 5 nm in diameter) immediately after introduction into the HRTEM column. Within 20 min under an electron beam bombardment (400 keV), crystallization started to occur, as shown in Figure 1d. Fresh WS_2 nuclei in various orientations were clearly observed, which indicates that curling of the crystallites has occurred during electron bombardment. A similar process for the generation of nested carbon fullerenes from amorphous soot was reported recently.⁸

STM analyses of MoS_2 films containing NP showed oval-shaped globules which were abundant on the sample surface, and barely any flat areas could be found. Some of the globules contained edges with well-defined apex angles (*vide infra*). These globules resembled in shape and size the NP examined earlier using TEM.^{2b} Two size distributions of MoS_2 NP were observed in distinctly separated zones: in one kind of zone, NP of 6×3 to 15×7 nm² in size were found; in other zones, NP with sizes 30×10 to 60×30 nm² were observed. NP of $MoSe_2$ and WSe_2 were also observed, although their fraction in the film was inferior to that of the sulfides. Figure 2a and b show MoS_2 and $MoSe_2$ NP, respectively. The insets of Figure 2 provide a vertical contour of the NP across its halfperimeter. The round contour and the measured (half) height of the NP are convincing evidence in support of the suggested oblate shape of the NP. The roughness of the vertical contour can be attributed to the "corona" which wraps the NP (Figure 1a). While most of the NPs are oblate or round, a few resemble a cigar or closed tubule (Figure 2c). To confirm that this latter shape is not an experimental artifact, scans in perpendicular directions were conducted and produced the same cigar-like shapes. The vertical contours in the plane perpendicular to its main axis confirm the round nature of the tubule shown in Figure 2c. The NP of MSe_2 were dispersed in an amorphous matrix, and further effort is necessary to increase the fraction of the NP phase in these materials.

MO_x samples which were heated to higher temperatures (>950 °C) in the same gas atmosphere yielded highly oriented platelets (c -axis perpendicular to the substrate ($\perp c$)) of the 2H- MX_2 phase. STM images of such MoS_2 samples were not different from the atomically resolved images reported by others.^{3,4} On the other hand, if the reaction was stopped after only a few minutes (≤ 850 °C), most of the material was still in amorphous form, as evidenced by TEM and XRD. Also, STM images could not be obtained with such samples, although the samples were flat. These observations indicate that the NP is an intermediate phase between amorphous MoS_x (or $MoOS_x$) and the crystalline 2H- MoS_2 phase. Wetting of the substrate by the NP seems to play an important role in determining the sizes of the NP. Nonpolar substrates, like the basal (vdW) plane of graphite or 2H- MoS_2 crystals, could lead to a more uniform size distribution, a topic currently under investigation in our laboratory.

In contrast with HRTEM observations, images with atomic resolution could not be obtained on the curved surfaces of the MX_2 NP and nanotubules with STM. Atomic resolution has not been reported with STM for both carbon fullerenes^{9–12} and nanotubules,¹³ nor has it been achieved with TEM.¹⁴ On the other hand, graphite, which can be regarded as the bulk precursor of carbon fullerenes, is used as a standard material for the

(8) Ugarte, D. *Nature* **1992**, *359*, 707.

(9) (a) Wilson, R. J.; Meijer, G.; Bethune, D. S.; Johnson, R. D.; Chambliss, D. D.; de Vries, M. S.; Hunziker, H. E.; Wendt, H. R. *Nature* **1990**, *348*, 621. (b) Wragg, J. L.; Chamberlain, J. E.; White, H. W.; Krätschmer, W.; Huffman, D. R. *Nature* **1990**, *348*, 623.

(10) (a) Lu, Y. Z.; Patrin, J. C.; Chander, M.; Weaver, J. H.; Chibante, L. P. F.; Smalley, R. E. *Science* **1991**, *252*, 547. (b) Li, Y. Z.; Chander, M.; Patrin, J. C.; Weaver, J. H.; Chibante, L. P. F.; Smalley, R. E. *Science* **1991**, *253*, 429.

(6) Kroto, H. W. *Science* **1988**, *242*, 1139.

(7) Bursill, L. *Int. J. Mod. Phys. B* **1990**, *4*, 2197.

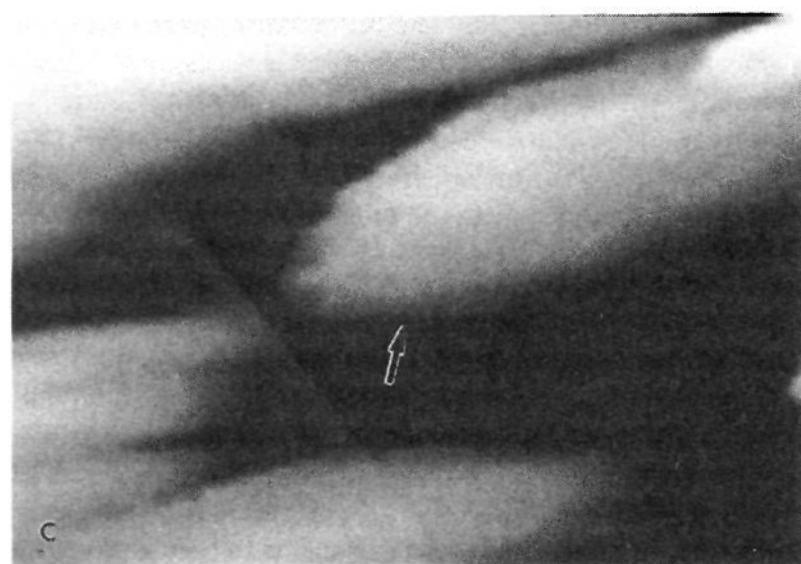
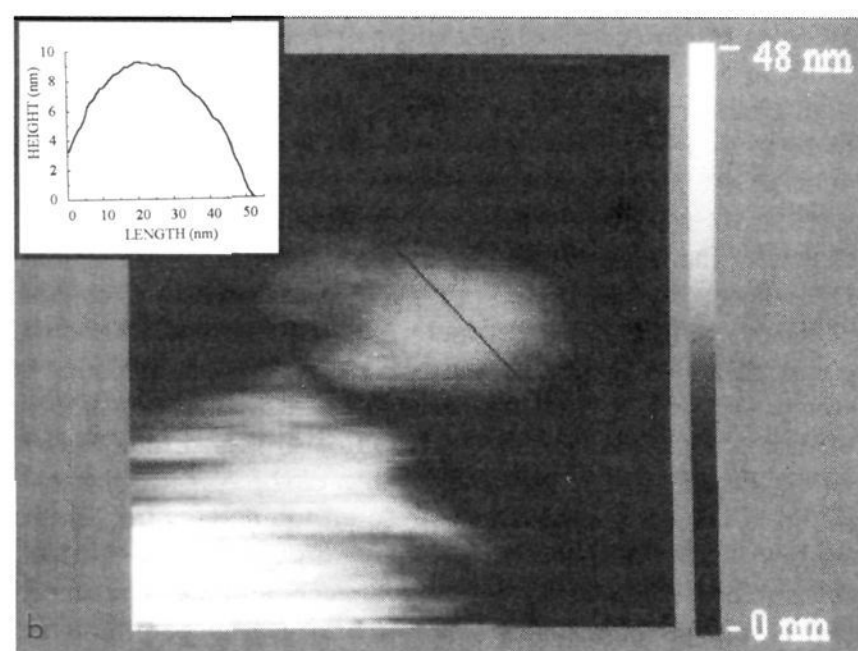
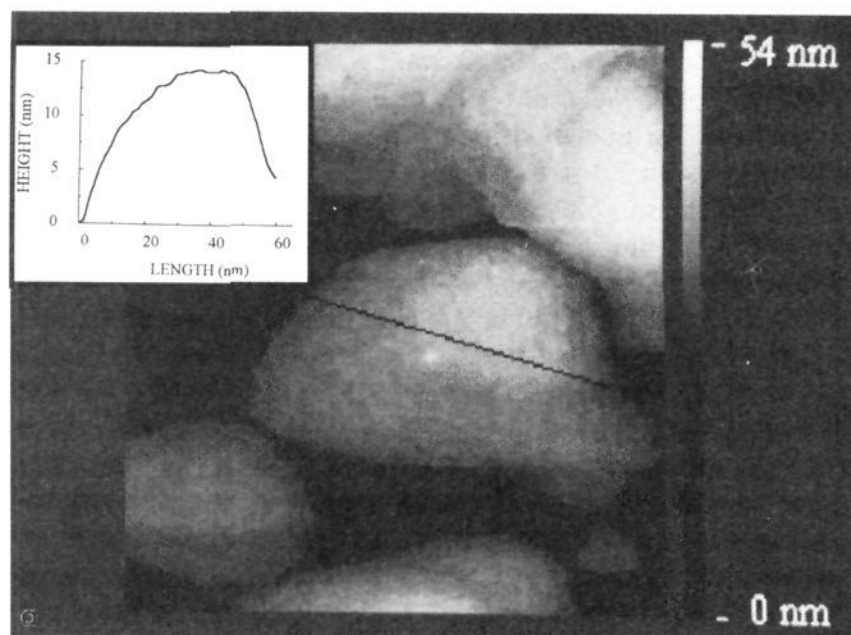


Figure 2. STM images of (a) ($85 \times 85 \text{ nm}^2$) MoS_2 and (b) ($103 \times 103 \text{ nm}^2$) MoSe_2 polyhedra. The vertical contour of each polyhedra between the two crosses is shown in the inset. The height is indicated by the gray scale on the right. (c) MoSe_2 tubule (flash) of ca. 100-nm diameter and 600-nm length.

calibration of atomically resolved STM (AFM). Recent experimental and theoretical works^{15,16} suggest that the charge density distributions of the highest occupied and the lowest unoccupied

(11) (a) Lamb, L. D.; Huffman, D. R.; Workman, R. K.; Howells, S.; Chen, T.; Sarid, D.; Ziolo, R. F. *Science* **1992**, *255*, 1413. (b) Chen, T.; Howells, S.; Gallagher, M.; Sarid, D.; Lamb, L. D.; Huffman, D. R.; Workman, R. K. *Phys. Rev. B* **1992**, *45*, 14411. (c) Howells, S.; Chen, T.; Gallagher, M.; Sarid, D.; Lichtenberger, D. L.; Wright, L. L.; Ray, C. D.; Huffman, D. R.; Lamb, L. D. *Surf. Sci.* **1992**, *274*, 141.

(12) Dietz, P.; Fostiropoulos, K.; Krätchmer, W.; Hansma, P. K. *Appl. Phys. Lett.* **1992**, *60*, 62.

(13) Zhang, Z.; Lieber, C. M. *Appl. Phys. Lett.* **1993**, *62*, 2792.

(14) (a) Iijima, S. *J. Cryst. Growth* **1980**, *50*, 675; (b) *Nature* **1991**, *354*, 56. (c) Buseck, P. R.; Tsipursky, S. J.; Hettich, R. *Science* **1992**, *257*, 215.

(15) Wang, X.-D.; Hashizume, T.; Shinohara, H.; Saito, Y.; Nishina, Y.; Sakurai, T. *Phys. Rev. B* **1993**, *47*, 15923.

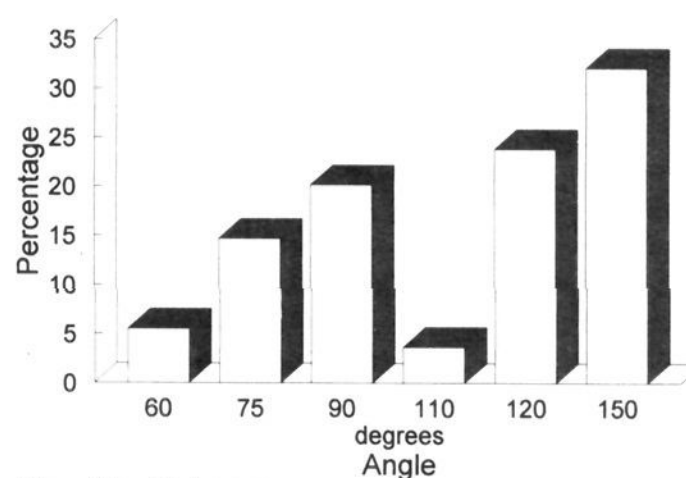


Figure 3. Histogram of the apex angles for NP with sharp corners (experimental error is $\pm 3^\circ$). A special procedure was used in order to ensure that the NP is not at an oblique angle relative to the substrate.

molecular orbitals of C_{60} are shaped like stripes, and hence STM with atomic resolution may not be observable at all. The fast rotation at room temperature and the curvature of the molecule surface could contribute to the fuzziness of the STM images of fullerites (however, rotation is not admissible for nanotubes). Some of these arguments could also explain the absence of atomic resolution in MX_2 NP. However, the most likely explanation for the lack of atomic resolution in the STM analysis is the existence of the "corona" which wraps the NP. This is supported by the fact that as soon as the material is annealed at temperatures $> 950^\circ\text{C}$, the entire material is transformed into highly oriented ($\perp c$) platelets of the 2H bulk phase, and atomic resolution is achieved.

To further study the structural properties, the apex angles of MoS_2 NP with sharp corners were determined by STM using a method which assured measurement of the proper apex angle and not its projection. The histogram of the apex angles, measured on 110 polyhedra with such sharp corners, is shown in Figure 3. The measured angles are in good agreement with the ones observed by TEM,^{2b} although the method of determination of the apex angle is not identical in the two techniques. The existence of apex angles $\leq 90^\circ$ may suggest that a triangle (60°) or rhombus (75° and 90°) is present on some apexes. Such polygons are part of the stable trigonal prismatic structure of MX_2 compounds, and hence they can exist in NP but not in carbon fullerenes.¹⁷ The folding of the hexagonal network in the apex may involve large geometrical constraints which are relieved by introducing a point defect (e.g., Mo vacancy) in the apex. Occasionally, an apex angle of 45° in NP was also observed by TEM.

Figure 4 shows some NP structures observed with TEM which were not reported hitherto. Figure 4a shows a WS_2 polyhedron whose projection is almost a perfect pentagon (top part). This NP is filled with a crystalline material. Other polyhedra, with nearly a perfect hexagonal shape in projection, were also identified. The bending of the atomic planes in each corner is very sharp and is likely to emanate from a point defect. Figure 4b shows a MoS_2 nanotubule, which is rather similar to the WS_2 nanotubules reported before.^{2a} NP of the metal diselenides were also identified by TEM. These images demonstrate the rich polymorphism which is manifested by these kind of materials.

The tunneling current was measured as a function of the applied potential (I-V curve) when the tip was fixed above a single NP of the kind shown in Figures 2a and b. In order to make sure that the I-V curve was taken on top of a NP, the measurement took place only after a small portion of the NP was scanned (zooming on). The voltage was varied between +2 and -2V. From the I-V curve a forbidden gap of ca. 1.1 eV for MoS_2 and 1.05 eV for MoSe_2 was estimated. These values represent a statistical average over 10 different measurements for each kind

(16) Kawazoe, Y.; Kamiyama, H.; Maruyama, Y.; Ohno, K. *Jpn. J. Appl. Phys.* **1993**, *32*, 1433.

(17) Kroto, H. W. *Nature* **1987**, *329*, 529.

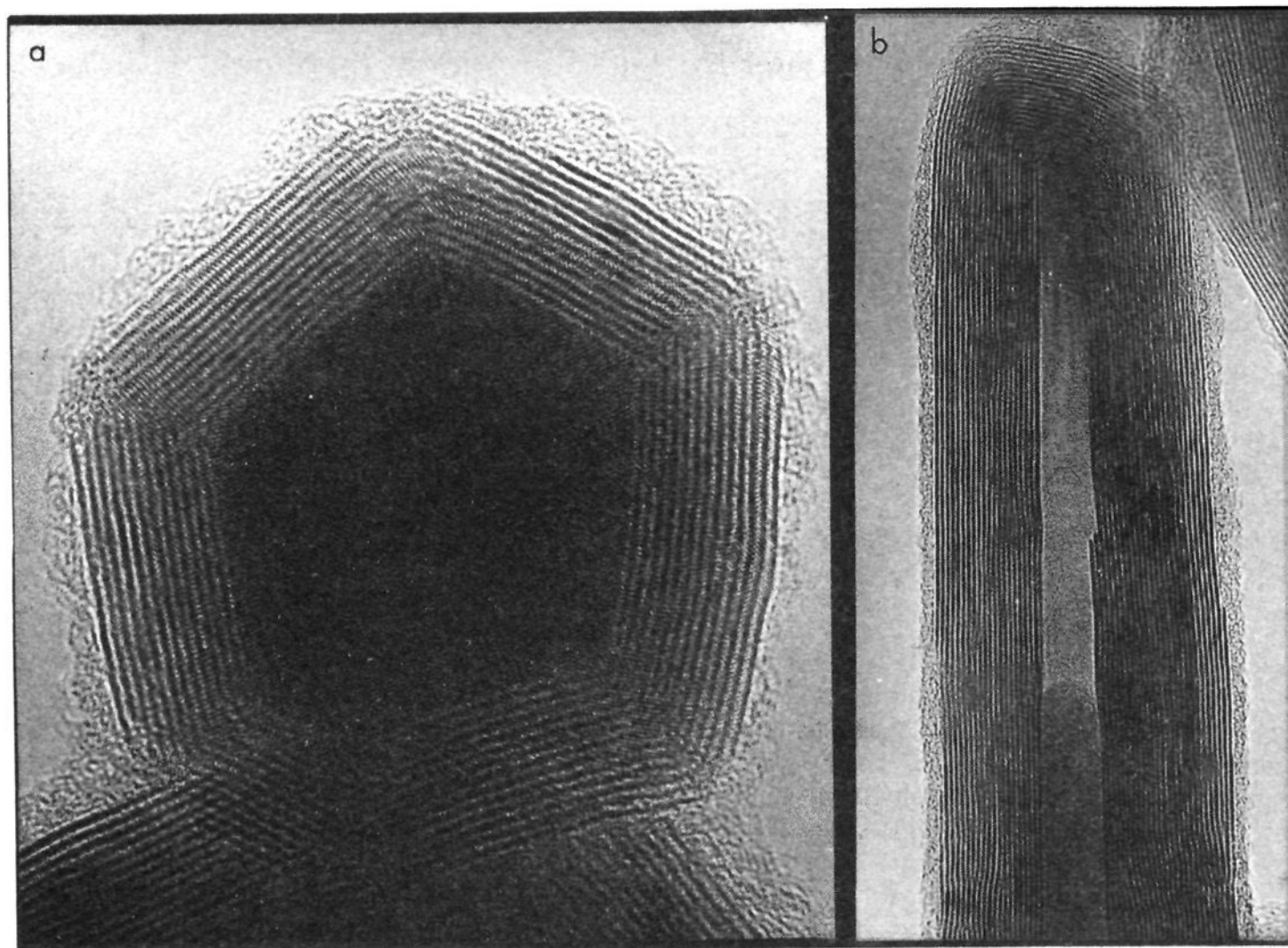


Figure 4. High-resolution images of NP structures. (a) WS_2 polyhedron with a pentagon-like structure at the top. (b) Nanotubule of MoS_2 . The average distance between each two fringes ($c/2$) is 0.62 nm.

of NP. This result strongly suggests that a NP of a size $20 \times 50 \text{ nm}^2$ is a semiconductor. The somewhat smaller gap of the NP, compared with the values of the bulk phase (1.2 eV for MoS_2 and 1.15 eV for $MoSe_2$),¹⁸ may be attributed to the expansion of $c/2$ (vdW gap) in various regions of the NP, due to the strain involved in the folding of the structure. An expansion of a few percent in $c/2$ of carbon nanotubes was also reported recently.¹⁹ An alternative explanation for the reduced gap of NP is that subbandgap states, which emanate from structural imperfections or edge dislocations, may serve as mediators for tunneling of charge and hence increase the current under bias.²⁰ The presence of the "corona" may also influence the measured bandgap of the NP. It can be anticipated, though it is not yet verified, that the bandgap of NP with a diameter $< 10 \text{ nm}$ will increase as a result of quantum confinement of the electrical charge.

Our experiments do not show any correlation between the presence of nanotubes and NP. Figure 1b shows that nanotubes do not serve as a precursor to the spontaneously growing polyhedra. Therefore, the mechanism for the growth of nested fullerenes from nanotubes, proposed earlier by Dravid et al.,²¹ can be precluded in the present case.

Recently, fibers and NP were found in amorphous boron nitride, which was heated to 1100°C .²² The stable form of boron nitride at room temperature is the hexagonal pseudographitic phase. This experiment further indicates that the thermodynamic stability of nanophases of 2D materials, which crystallize from an amorphous matrix, can be markedly different from those of the bulk phase, which leads to closed fullerene-like structures. More recently, carbon-free fullerenes were reported from intermetallic

compounds,²³ showing the large diversity of materials which exhibit fullerene-like structure.

A striking analogy exists between the series of transformations occurring in 2D materials shown here and the solidification of various metallic alloys, such as the Al-Mn, which exhibit the metastable quasicrystalline phase (QC) with icosahedral symmetry.²⁴ Thus, the QC phase can be obtained from the amorphous alloy upon heating, ion beam bombardment, or any equivalent form of energy input. Further heating of the QC phase transforms it into the stable bulk crystalline phase. Alternatively, the QC phase can be obtained by a rapid quenching of the melt. This analogy suggests not only that metastable phases with unique symmetries are quite abundant in nature but also that NP can possibly be obtained by quenching the melt of layered-type materials. However, not all such 2D materials are stable in the molten form; some, like WS_2 , decompose prior to melting.

In conclusion, high-resolution TEM and STM were used to study the growth mechanism of nested polyhedra (fullerene-like) structures of some layered dichalcogenide semiconductors. NP and nanotubes were observed in metal diselenides, and new structures (polyhedra with pentagon- or hexagon-like shape in projection) were identified. Spontaneous and electron beam assisted growth of the NP from amorphous precursor was observed. The analogy with the growth mechanisms of other nanophase materials was discussed.

Acknowledgment. We are grateful to Dr. G. Salitra for preparation of some of the samples used in this research. This work was supported by grants from the New Energy Development Organization of Japan; the Israeli Ministry of Energy and Infrastructure, and the Israeli Ministry of Science and Technology.

(18) Kam, K. K.; Parkinson, B. J. *J. Phys. Chem.* **1982**, *86*, 463.

(19) Saito, Y.; Yoshikawa, T.; Bandow, S.; Tomita, M. *Phys. Rev. B* **1993**, *48*, 1907.

(20) Parkinson, B. A.; Furtak, T. E.; Canfield, D.; Kam, K.; Kline, G. *Faraday Discuss. R. Soc. Chem.* **1980**, *70*(23), 1.

(21) Dravid, V. P.; Lin, X.; Wang, Y.; Wang, X. K.; Yee, A.; Ketterson, J. B.; Chang, R. P. H. *Science* **1993**, *259*, 1601.

(22) Hamilton, E. J. M.; Dolan, S. E.; Mann, C. M.; Colijn, H. O.; McDonald, C. A.; Shore, S. G. *Science* **1993**, *260*, 659.

(23) (a) Winters, R. R.; Hammack, W. S. *Science* **1993**, *260*, 202. (b) Sevov, S. C.; Corbett, J. D. *Science* **1993**, *262*, 880.

(24) (a) Schechtman, D.; Blech, I.; Gratias, D.; Cahn, J. W. *Phys. Rev. Lett.* **1984**, *53*, 1951-1954. (b) Kaufman, M. J.; Biancanello, F. S.; Kreider, K. G. *J. Mater. Res.* **1988**, *3*, 1342. (c) Wang, Y.; Wu, Z. *Proc. Conf. Crystallogr.*, **13th** 1988 205; *Chem. Abstr.*, **1991**, *114*, 190419.